Nonintrusive appliance load monitoring (NIALM) for energy control in residential buildings

Michael Zeifman, Craig Akers, Kurt Roth

Fraunhofer Center for Sustainable Energy Systems

Abstract

Significant saving in energy consumption can be achieved by better energy management and control in residential buildings. More advanced control approaches require real-time information on the appliances in use. A straightforward method to obtain this information uses a power sensor attached to each household appliance of interest. Unfortunately, this method is costly and requires significant installation and maintenance efforts. A more sophisticated way to obtain appliance-specific data is by disaggregation of total power consumption data acquired at the main breaker level. Such nonintrusive appliance load monitoring (NIALM) uses a single point of power measurement (e.g., of the electric feed for the whole house), combined with special signal processing techniques.

Our paper presents overviews and test results for two novel NIALM approaches we are developing and testing. The first system uses an inexpensive off-the-shelf sensor (TED – The Energy Detective) to obtain real power data at a 1 Hz sampling rate. A statistical algorithm, optimally implementing historical data on power draws and power consumption patterns, has been developed for this system. The algorithm is capable of semi-automatic detection of major household appliances and outperforms the known NIALM algorithms in terms of detection accuracy. The second system relies on a custom-built sensor capable of sampling voltage and current at a rate of up to 100 kHz. At this sampling rate, voltage and current waveforms and their features are used to identify and track a much broader range of household appliances.

1. Introduction

Recent studies indicate that providing a consumer with a continuous feedback on the household appliance-specific power draw can lead to significant energy saving [1]-[6]. Such feedback can be based on continuous monitoring of household appliances. By attaching a sensor or a communication device to each appliance, it is possible to collect and disseminate the power-draw information in near real time [7]. Coupled with the Smart Grid, these “smartened” appliances could also be used in home automation networks [7]. However, as van Elburg pointed out, this option is “relatively expensive and complicated to supply” [4]. Moreover, many customers object to the modification of household appliances and home automation networks [7].

A nonintrusive appliance load monitoring (NIALM) method that uses a single point of power measurement (e.g., the electric feed for the whole house) can enable an alternative feedback option. Such a method requires both hardware (a sensor) and software (signal processing algorithms) components. The software component of NIALM depends on the hardware implementation. For example, signal waveform analysis can be used if the sensor samples voltage and current at a rate of at least several kHz. However, such sensors are still expensive and less available. An inexpensive and easy-to-install hardware alternative is a sensor that measures the total electric power in a residential unit at a sampling frequency of about 1 Hz.

We have conducted an extensive review of the existent NIALM systems and algorithms [8] and concluded that (i) existent NIALM methods are either not robust or provide marginal accuracy (~80%), and (ii) potential improvement can be achieved by using additional information and/or by combining several different methods. In this paper, we have applied these conclusions in two different sets of algorithms. In the first algorithmic set, we use statistics of time on, time off and power surge to complement the information on the power changes. This set is suitable for the low-frequency sensors. In the second set, we optimally combine two different algorithms that utilize signal waveform features. This set is intended for the high-frequency sensors.

The paper is organized as follows. Section 2 gives a brief overview of a NIALM system. The NIALM method we developed for a low-frequency sensor is presented in Section 3. By using simulation

examples, we demonstrate that this method has the potential to outperform existent methods. In Section 4, we present our NIALM method for high-frequency sensors. The method combines together a multivariate statistical technique and a pattern recognition technique. The method is tested using our laboratory system. The two developed NIALM methods can be combined together in the future work, which is briefly discussed in Section 5.

2. NIALM Overview

The main idea of NIALM is to obtain appliance-specific information nonintrusively. The information is collected at the main breaker level (or at a circuit breaker level), and then disaggregated to obtain operational time and power draw information. Figure 1 shows an example of an aggregated power signal and the corresponding NIALM solution. In this illustration, the reconstructed operational time of e.g., a TV, is from 7:20 AM to about 8:30 AM, and the power draw is about 300 W.

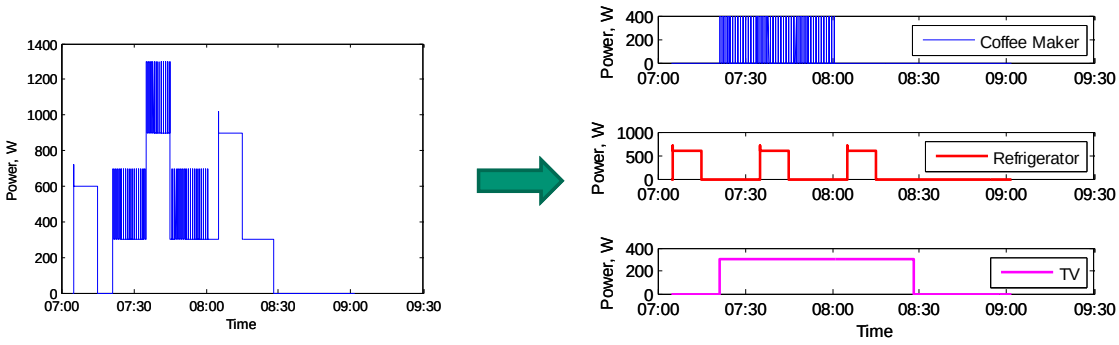

Figure 1. NIALM disaggregates an overall signal (left) into the loads on individual appliances.

In this illustrative example, the appliances are modeled as on/off appliances that consume constant power at a single steady state. In reality, coffeemaker loads depend on the water volume, TV power draw often follows the volume/brightness levels, and refrigerators have a second power state corresponding to defrosting. To encompass the variability in appliances' power draw patterns, the following four groups are suggested [9]:

1. **Permanent consumer devices**. Consumer devices that remain on for 24 hours a day, 7 days a week, with approximately constant active and reactive power draw. Examples of devices in this category include hard-wired smoke alarms and some external power supplies.

2. **On-off appliances**. Most household appliances, such as a toaster, light bulb, or water pump belong to this category.

3. **Finite state machines (FSM) or multistate devices**. This category includes consumer devices that pass through several definite switching states, whereby the complete switching cycle is repeated frequently in the daily or weekly cycle of events. Examples of FSM are a washing machine or clothes dryer.

4. **Continuously variable consumer devices**. Consumer devices with variable power draw, with no any periodic pattern of changing the states or power. Examples of such appliances include dimmer lights and power tools.

The NIALM example shown in Figure 1 is related to the low-frequency sensors that sample real and/or reactive power components. The underlying NIALM algorithms can only implement "macroscopic" signal features, e.g., changes in power draw. As such, the group of NIALM algorithms that utilize the low-frequency sensor signals is successful with on-off appliances that have significantly different power draws at the steady state. Use of the "microscopic" features of signals obtained with the high-frequency sensors can potentially help detect other groups of appliances.

3. NIALM Method for low sampling rate

Inexpensive and easy to install energy monitoring systems such as, e.g., the Energy Detective (TED) [10] and the corresponding Google Power Meter [11] can be used for NIALM. TED (see Figure 2) can record the real power and voltage at 1 Hz frequency and the Power Meter can display this information over the Internet. NIALM algorithms suitable for such a sensor have been detailed in several publications [9], [12]-[15]. These algorithms detect step changes in power and match these changes with the appliances being turned on or off.

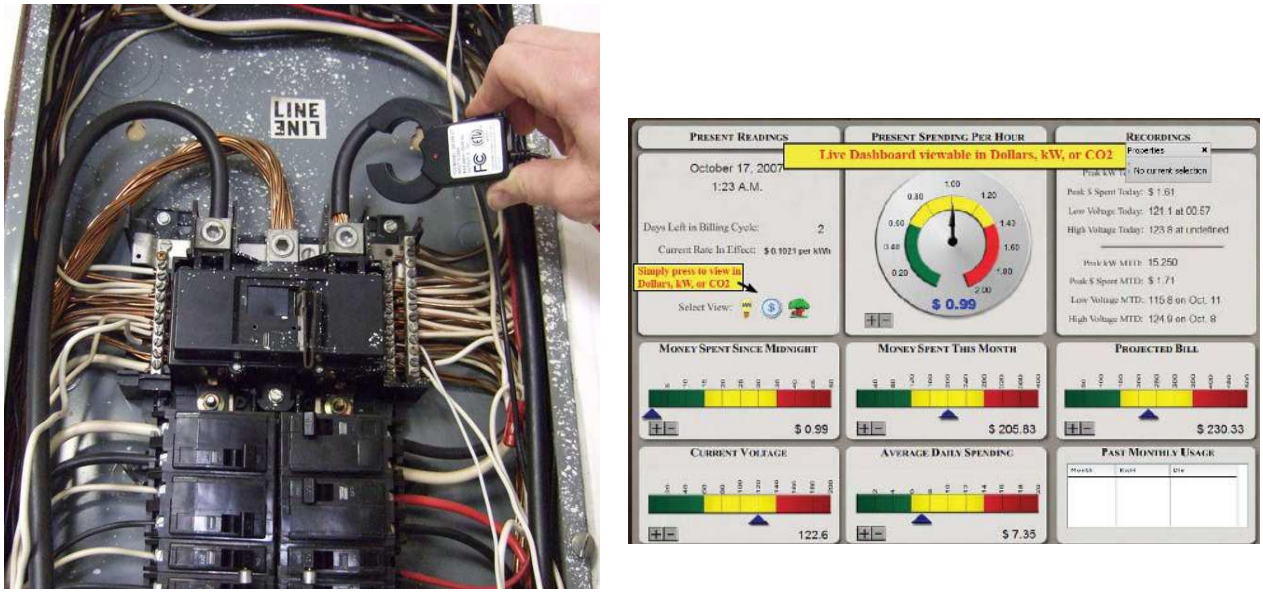

Figure 2. The Energy Detective (TED). Left: Current transformer of TED. Right: TED dashboard. From [10].

Even though these NIALM algorithms are capable of monitoring major household appliances, their accuracy level is of the order of 80%. The main reason for this marginal monitoring accuracy is an overlap in the power draw between different appliances. For example, the power draw of a computer monitor could equal that of an incandescent bulb, which makes these two appliances undistinguishable for the mentioned algorithms.

Our NIALM algorithm can overcome this challenge. There are three main novelties in our algorithm. First, not only power changes but also power surges (statistics of surge amplitude and duration) and their statistical distributions are used in order to better segment the appliances. Second, statistics of time of use (in terms of both duration and time of day) are included for better appliance separation. Third, the matching between the measurable power observations and the appliances is made by considering a series of transitions among the appliance states that maximizes the likelihood of not only the given series of power changes but also the time-of-use statistics and power surge statistics.

The algorithm is explained in detail elsewhere [16]. Here, we provide a brief overview. Figure 3 shows power-related features we use in the algorithm. The statistics of these features can be obtained by collecting and analyzing historical data. Similarly, the time duration statistics, i.e., the distributions of time on and time off for appliances can also be obtained. A combined cluster and statistical analysis is implemented in order to split the distributions that apparently involve more than one appliance or to merge the distributions corresponding to the same appliance. These analyses are continuously updated as new data are collected.

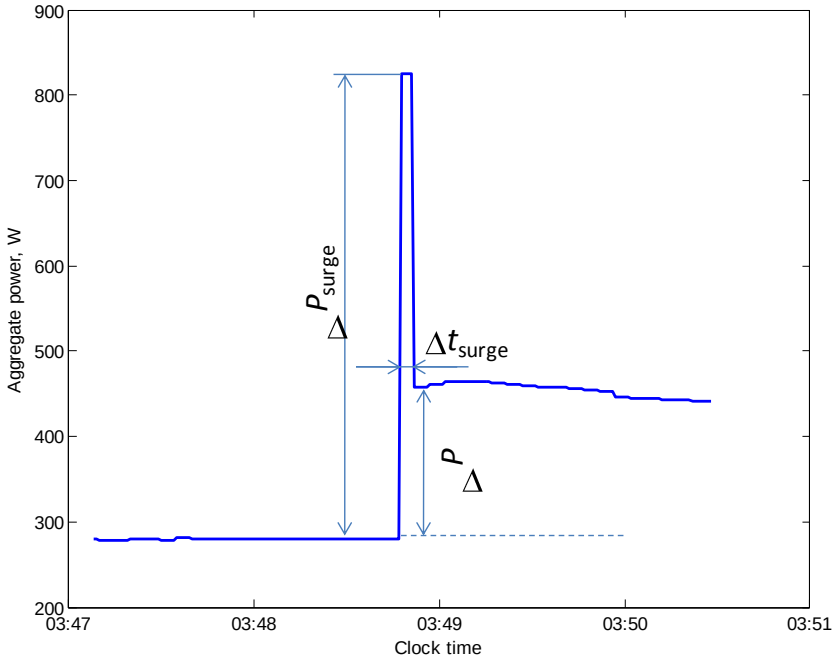

Figure 3. Power-related features: ΔP_{surge} is the power surge amplitude, ΔP is the change of steady-state power and Δt_{surge} is the surge duration in time.

Once the main appliances in a household are identified and characterized by the historical data, the main algorithm can process the new data by calculating the most likely path of appliance state changes (i.e., transitions) over time. We realize this by a Viterbi-type algorithm. Since the common Viterbi algorithm considers all possible transitions within a system, the system size (in our case, this equals the number of appliances in a household) renders a common Viterbi algorithm not amenable for computation. We have overcome this challenge by considering pairs of appliances with similar power draw. The resultant Viterbi algorithm with Sparse Transitions (VAST) has a computational complexity that is linearly proportional to the number of appliances, whereas a common Viterbi algorithm's complexity would exponentially grow with the number of appliances.

Figure 4 shows a principal block-scheme of our algorithm. The algorithm uses sensor measurements to calculate candidate times on and off. Subsequently, all these data are used by the algorithm to calculate the likeliest transition path, using the transition probabilities that are estimated by the prior statistics. These statistics are continuously updated by the new data.

We expect our algorithm to perform better than other algorithms for appliances with overlapping power draw. To test its performance, we consider simulated data on two appliances with a heavy overlap between the power draws [16]. The simulation data include 300 positive and 300 negative changes of power accumulated over 10 hours of sampling with 1 Hz frequency for two such appliances. The distributions of the power draw of the two appliances are Gaussian with means of 130W and 150 W for positive power changes and of -135W and -160W for negative power changes and standard deviations of 15W and 20W respectively. The distributions of time-on durations are uniform with boundaries of 30s and 80s for the first appliance and of 60 s and 100 s for the second appliance. Figure 5 plots the probability density functions (PDF) of the power draw, and clearly shows the heavy overlap in power draw between the appliances.

Figure 6 displays a fragment of the data generated along with the indication of appliance states. The indicator takes value 1 if appliance 1 is turned on, value 2 if appliance 2 is turned on, value -1 if appliance 1 is turned off, and value -2 if appliance 2 is turned off. Clearly, the heavy overlap between the power draws of the two appliances makes the reconstruction of appliance states a challenging problem.

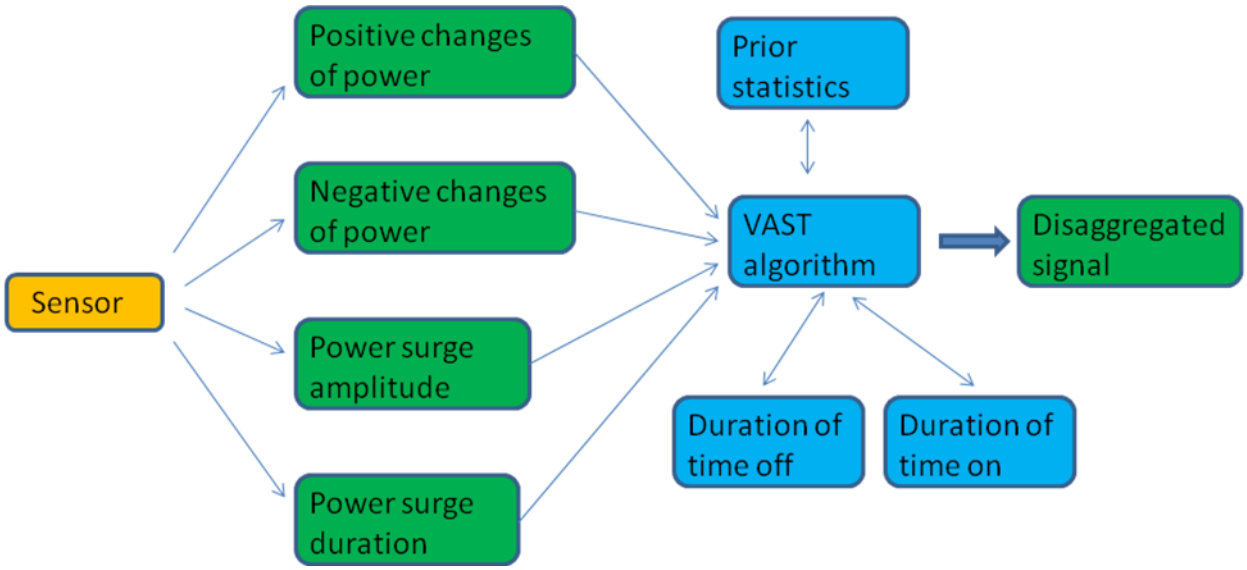

Figure 4. Block-scheme of our algorithm

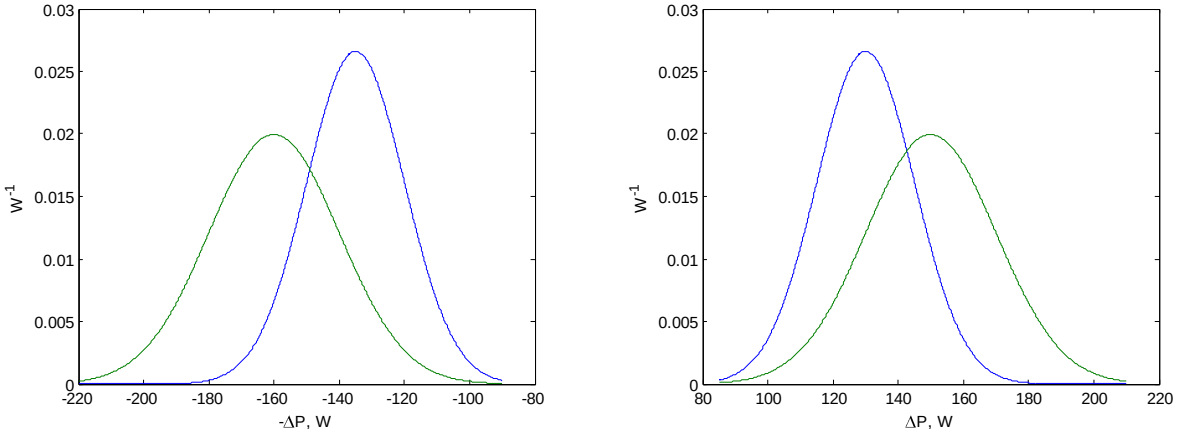

Figure 5. PDFs of negative (left) and positive (right) changes of power used in simulation of two appliances. From [16]. © 2011 IEEE

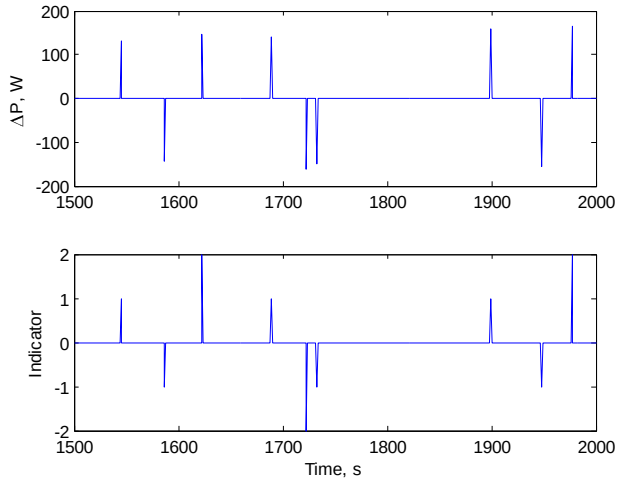

Figure 6. Fragment of simulated data. Total data set includes 600 power changes over 10 hours. From [16]. © 2011 IEEE

Firstly, we apply a common NIALM algorithm [9] to the simulated data. Portion of the results that correspond to the data fragment of Figure 6 are shown in Figure 7. The indicator takes value 0 whenever no matching between the positive and negative power changes of the same appliance can be found. It is seen in the Figure that the common algorithm performs poorly. The overall fraction of correctly reconstructed appliance states is 54.5%.

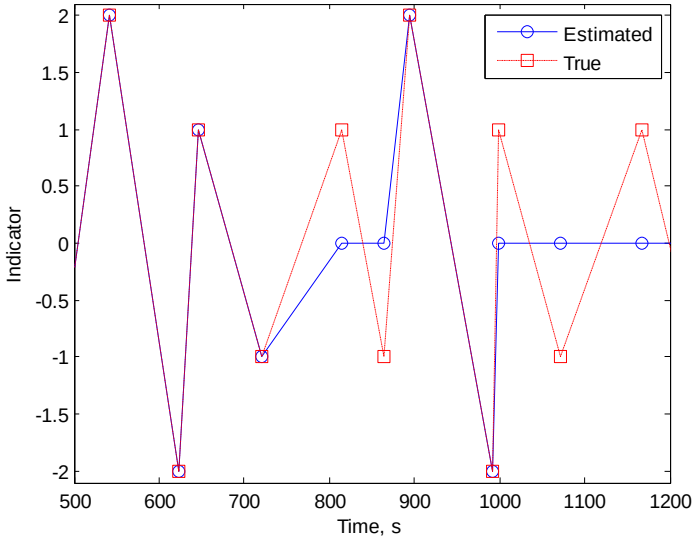

Figure 7. Fragment of results of established NIALM algorithm, applied to simulation data. Overall correct reconstruction is 54.5%. From [16]. © 2011 IEEE

The results of our VAST algorithm, applied to the simulated data, are shown in Figure 8. This particular portion of results indicates a perfect restoration of the appliance states. The overall fraction of correctly reconstructed appliance states for the proposed algorithm is 97.3%. This is a dramatic improvement over the conventional method.

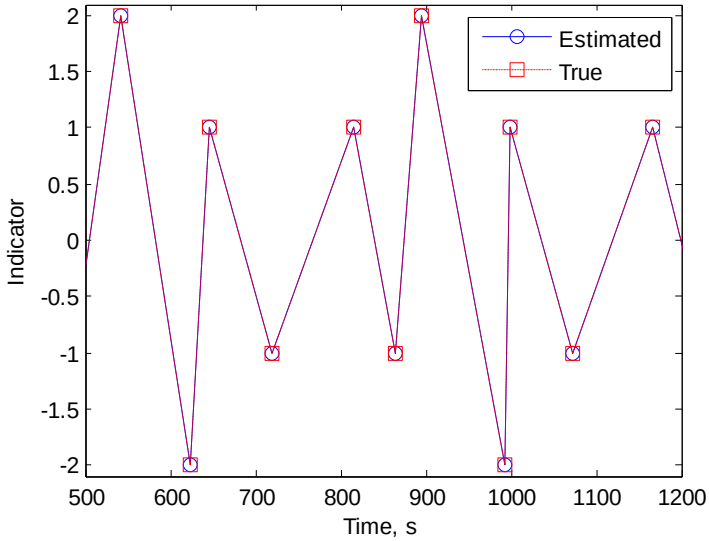

Figure 8. Fragment of results of our VAST algorithm, applied to simulation data. Overall correct reconstruction is 97.3%. From [16]. © 2011 IEEE

4. NIALM Method for high sampling rate

Signals sampled with a rate of more than several kHz can be used for waveform characterization. The use of waveform “microscopic” features can improve NIALM accuracy. In fact, the reported accuracy

of NIALM methods based on high-frequency sampled signal is of the order of 90% [8]. Further improvement of accuracy can be achieved by combining two or more different methods based on different features [8]. In this Section, we describe our experimental data acquisition system and a proposed set of two combined algorithms for NIALM.

4.1 Data Acquisition System

Based on the results of the literature review [8], we decided to start exploring high-frequency NIALM with a sampling rate of 500 kHz. At these high sampling rates, data transfer and storage pose a challenge, since the data file size reaches tens of MB even during a 1s sampling period. Since the appliances need to be characterized not only in a steady-state regime but also in transitions from one regime, e.g., standby, to another regime, e.g., power on, there is a need to automatically identify such transitions and record the data accordingly.

The above challenges have been overcome in the system we call the iMEL-C (Individual Miscellaneous Electric Load Characterization System). The iMEL-C consists of a Data Acquisition device, a signal interface device, and software that runs on a Windows based laptop computer. The selected Data Acquisition (DAQ) device is the National Instruments USB-6251. It is an externally powered, USB DAQ device with 16bit resolution, multiple input ranges and a maximum sampling rate of 1MHz (aggregate) while sampling multiple channels.

The Signal Interface consists of current censors, a voltage sensor (voltage divider), a power supply for the current sensors, fuses, a devise under test (DUT) power switch and an enclosure. Figure 9 shows a photograph of iMEL-C, an explanation of the PCB layout follows.

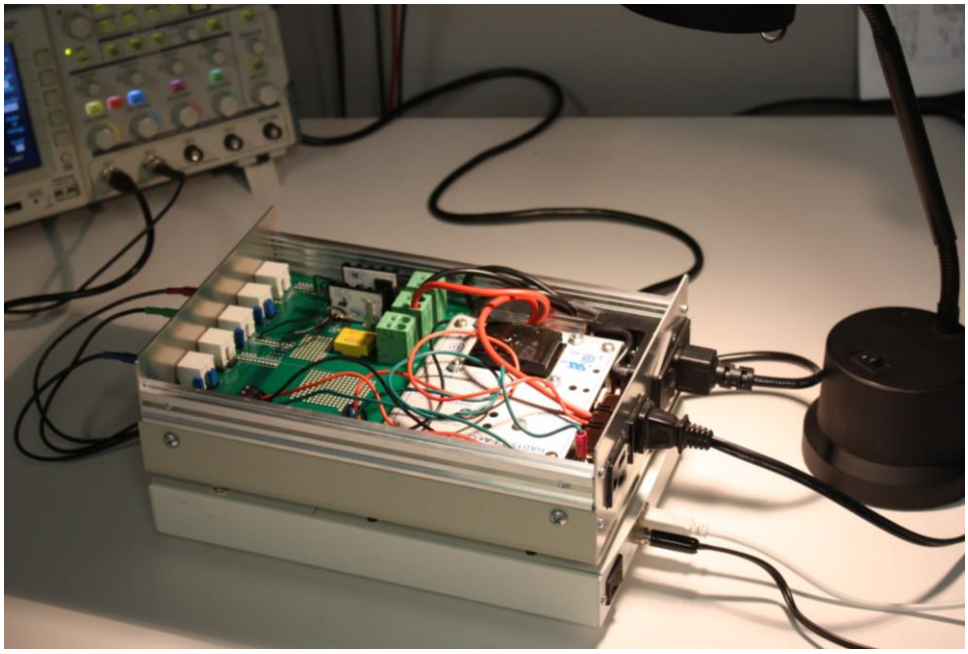

Figure 9. iMEL-C system for data acquisition

Voltage Sensor:

The voltage sensor consists of a voltage divider made of a 100kOhm resistor and a 1kOhm resistor. The measured reduction factor from the voltage divider is 0.982%. The DAQ system differential input impedance paths are significantly higher (rated at 10GOhm from input to DAQ ground) so no appreciable error is introduced through the DAQ. The voltage divider is jumper configurable between Load and Neutral, Load and Ground, or Neutral and Ground.

The voltage sensor circuit is independently fused with a fast-acting low current fuse, in case of a short in the system.

Current Sensor:

The iMEL-C system has three current sensors: one F.W. Bell NT-5 Magneto-Resistive Sensor, one F.W. Bell NT-15 Magneto-Resistive Sensor, and one Sensitec CDS4015 Magneto-Resistive Sensor. Although we performed tests with each sensor, we used the NT-15 for the 500kHz high frequency load characterizations because it has a good current range, over current protection, and good sensitivity at low currents.

Signal Interface:

The signal interface device consists of an enclosure that houses the electronic components of the system. It includes a linear (low ripple) DC power supply, to power the current sensors, a standard outlet receptacle, to plug electric devices into, a power switch with two fuses (one for the power supply, and one for the voltage sensor circuit), and a custom PCB containing the interface circuits for the voltage and current sensors, and additional circuits for grounding and isolation options of the output signals, to ensure a proper interface to the DAQ device. The PCB also includes expansion sites to accommodate further potential circuit configurations, such as notch filters or low pass filters.

4.2 Algorithms and results

Our high-frequency algorithms are based on the detection of transients in the waveform. Whenever the system observes a statistically significant change in the waveform, it records several waveforms before and after the change. It obtains the waveform of an appliance that apparently changed its state by subtracting the waveform before the change from that after the change. Figure 10 shows typical waveforms obtained in this way. Note that the waveforms are noisy and quite variable due to different appliance states. Note also that a waveform of Luminaire lamp (panel C on Figure 11) can be very close to that of the fan (panel D).

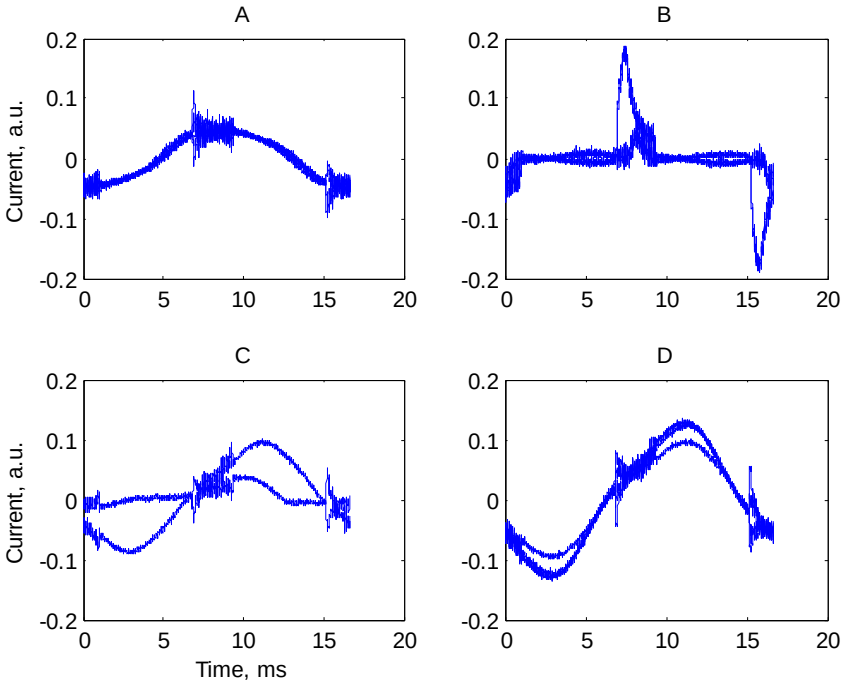

Figure 10. Waveforms of CFL lamp (A), CRT TV (B), incandescent special lamp Luminaire (C) and fan (D) in different setting. The waveforms are obtained by subtraction of a steady-state waveform before and after a transient detection. The transient can be either turning on or off.

Our two algorithms use waveform harmonics and a multivariate technique based on an unprocessed waveform. To combine these algorithms together, we implemented a probabilistic setting for each. In this setting, a PDF underlying an algorithm is calculated for an experimental waveform using previously obtained PDF-s for waveforms of all appliances. The experimental waveform is then classified based on the maximum PDF value.

This approach is illustrated in Figures 11 and 12. We used a sequence of 17 transitions (on/off) among the four appliances and calculated a PDF value for each experimental waveform on the basis of the PDF-s of the four appliances. In this way, we obtained 68 PDF values, four for each transition. The appliance state is then reconstructed using the maximum PDF value for each of the 17 transitions. It can be observed that algorithm based on waveform harmonics produces one wrong classification whereas the multivariate statistical technique perfectly classifies the appliances.

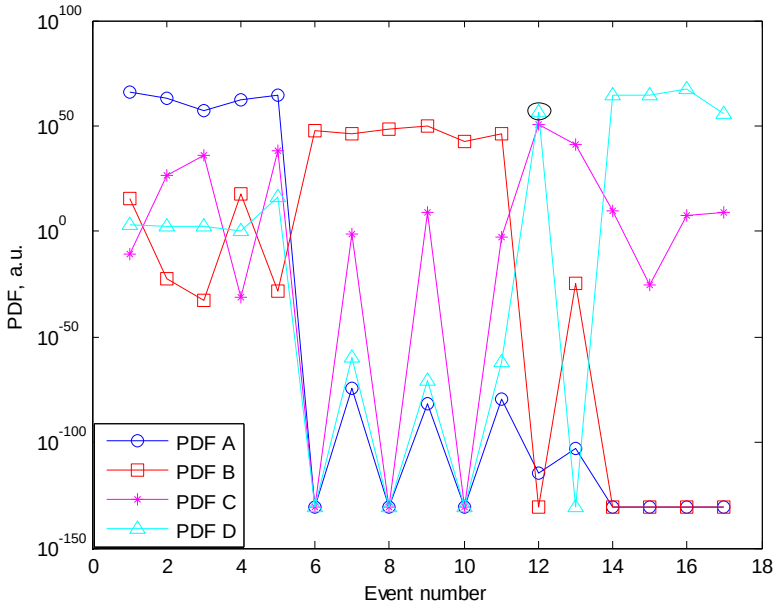

Figure 11. PDF-s corresponding to our algorithm that is based on waveform harmonics, the classification is based on the maximum PDF value for each event. The actual event sequence is: A (1-5), B (6-11), C (12-13) and D (14-17). The wrong classification for event 12 is marked with an ellipse.

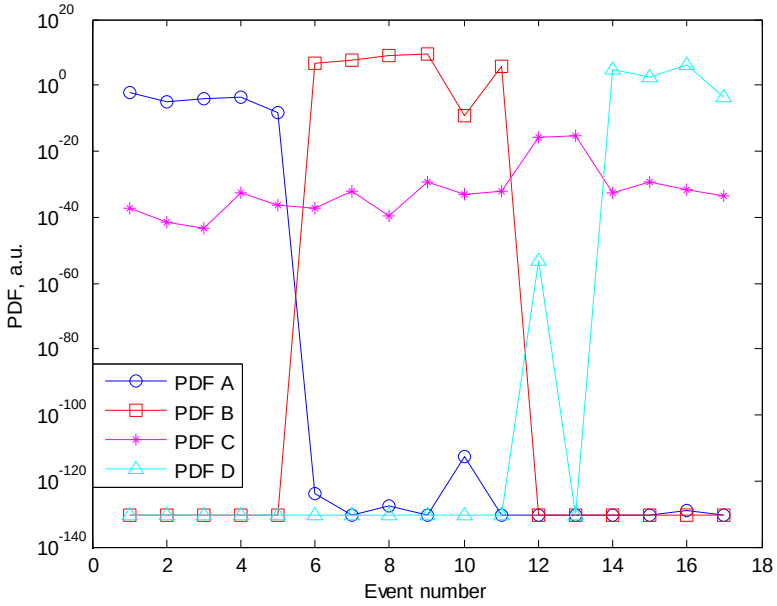

Figure 12. PDF-s corresponding to our algorithm that is based on a multivariate statistical technique, the classification is based on the maximum PDF value for each event. The actual event sequence is: A (1-5), B (6-11), C (12-13) and D (14-17). The wrong classification for event 12 is marked with an ellipse.

Figure 13 shows the results of the combined method; the combined method also detects 100% of appliances in this series.

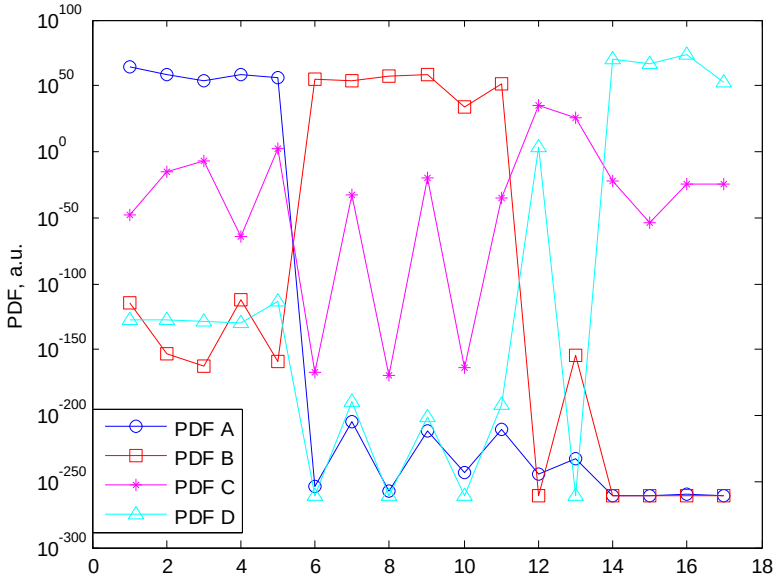

Figure 13. PDF-s corresponding to the combination of two algorithms, the classification is based on the maximum PDF value for each event. The actual event sequence is: A (1-5), B (6-11), C (12-13) and D (14-17). The wrong classification for event 12 is marked with an ellipse.

Finally, we used our iMEL-C system to follow the four appliances during an eight-hour period. During this time, we turned on and off the appliances and manually recorded the corresponding events. In total, there were 31 such events. After that, we applied our algorithms to reconstruct the appliance states. Figures 14 and 15 show the results.

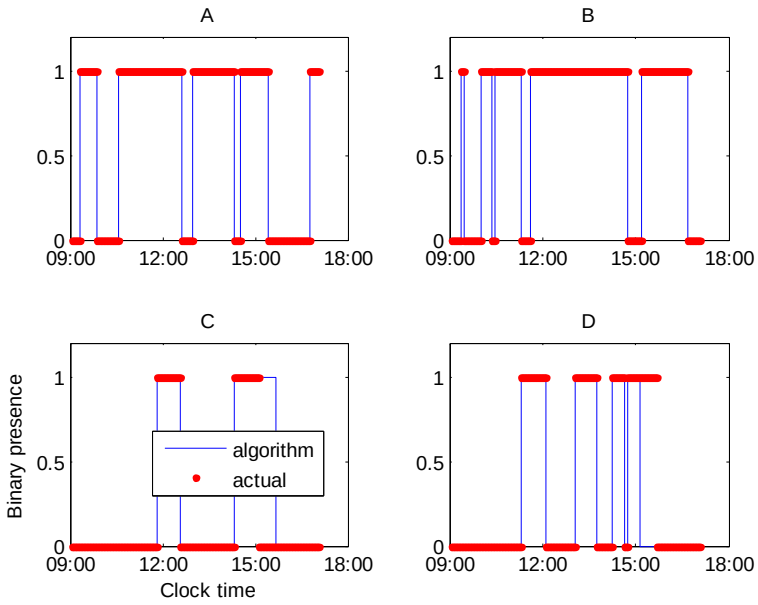

Figure 14. Disaggregation results for our harmonics-based algorithm. Appliances: CFL lamp (A), CRT TV (B), incandescent special lamp Luminaire (C) and fan (D).

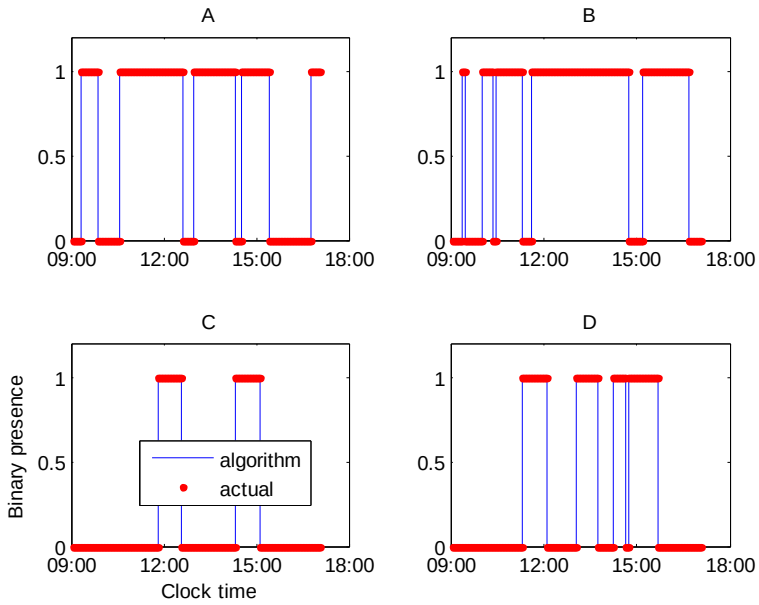

Figure 15. Disaggregation results for our multivariate-statistics algorithm and for the combined algorithm. Appliances: CFL lamp (A), CRT TV (B), incandescent special lamp Luminaire (C) and fan (D).

Figure 14 suggests that one transition was classified wrongly, so that the accuracy of the harmonics-based algorithm can be estimated as 30/31 = 96.8%. Both the algorithm based on a multivariate statistical technique and the combined algorithm provide a perfect reconstruction (100% accuracy), as can be seen in Figure 15.

5. Conclusions and Future Work

We have presented two different NIALM methods suitable for two different sensor types. The method suitable for a low-frequency sensor outperforms the existent NIALM method for the on/off appliances and, potentially, for the multistate appliances. Its accuracy for the simulated data is about 97%. The method suitable for a high-frequency sensor attains 100% disaggregation accuracy for the limited experimental data we collected.

In future work, we will further develop the first method and apply it to real data. We are currently monitoring two households using TEDs, and we will use the obtained data to benchmark our VAST algorithm. Since this algorithm involves transition probabilities, it can be combined with our second method that uses probabilistic pattern recognition. In this way, we can improve the accuracy and robustness of our approach.

Further, we expect to extend our approach to the permanent and variable-load appliances. The NIALM solution methods proposed for these appliances [8] can be implemented and combined with our main approach.

Acknowledgement

This work was supported in part by the U.S. Department of Energy under a subcontract with Lawrence Berkley National Laboratory number 6926442. We are grateful to Rich Brown of LBNL for helpful discussions.

References

[1] Darby S. *The effectiveness of feedback on Energy Consumption. A review for DEFRA of the literature on metering, billing and direct displays*, Environmental Change Institute University of Oxford, 2006.

[2] Gölz, S., Götz, K., Deffner, J. *Smart Metering – a means to promote sustainable energy consumption? Socio-technical research and development on feedback systems*, Proc. of the EEDAL-2009, p. 3.

[3] Likkanen, L. A., *Extreme-user approach and the design of energy feedback systems.* Proc. of the EEDAL-2009, p. 23.

[4] Van Elburg, H. *Encouraging public support for smart metering via appealing and enabling in-home energy feedback devices*. Proc. of the EEDAL-2009, p. 57.

[5] Pedersen P.E. *Impartial quality tests of compact fluorescent lamps*. Proc. of Right Light 4 (Copenhagen, Denmark, 19-21 Nov. 1997). ISBN 87-87071-73-8. Can be ordered from Borg&Co AB Services.

[6] Ehrhardt-Martinez, K., K.A. Donnelly, and J.A. Laitner, *Advanced Metering Initiatives and Residential Feedback Programs: a Meta-Review for Household Electricity-Saving Opportunities*, Report E105, ACEEE 2010.

[7] Lipoff, S., *Home Automation – the Unrealized Promise*, IEEE Consumer Electronics Society Newsletter, pp. 13-14, Fall 2010

[8] Zeifman, M., Roth, K., *Nonintrusive Appliance Load Monitoring: Review And Outlook*, Proceedings of IEEE Conference on Consumer Electronics, p. 243, 2011.

[9] Hart, G. W., *Nonintrusive Appliance Load Monitoring*, Proceedings of the IEEE, Vol. 80, pp. 1870-1891, 1992.

[10] www.theenergydetective.com

[11] www.google.com/powermeter

[12] Drenker, S., *Nonintrusive Monitoring of Electric Loads*, IEEE Computer Applications in Power, p. 47, 1999.

[13] Albicki, A. . and A. Cole, *Algorithm for Non-Intrusive Identification of Residential Appliances*, Circuits and Systems, Proceedings of the IEEE International Symposium on, Vol. III, pp. 338-341, 1998.

[14] Baranski, M., J. Voss, *Non-Intrusive Appliance Load Monitoring Based on an Optical Sensor*, EEE Power Tech Conference, Bologna, 2003.

[15] Matthews, H. L., *Automatically Disaggregating the Total Electrical Load in Residential Buildings: a Profile of the Required Solution* Intelligent Computing in Engineering - ICE08, 2008.

[16] Zeifman, M., Roth, K., *Viterbi Algorithm with Sparse Transitions (VAST) for Nonintrusive Load Monitoring*, Proceedings of IEEE Symposium on Computational Intelligence, 2011 (in press).